

# Critical Slowing Down of Triangular Lattice Spin-3/2 Heisenberg Antiferromagnet $\text{Li}_2\text{RuO}_6$ via $^7\text{Li}$ NMR

Yutaka ITOH<sup>1</sup>, Chishiro MICHIOKA<sup>1</sup>, Kazuyoshi OSHIMURA<sup>1</sup>,  
Kanao NAKAJIMA<sup>2</sup>, and Hirohiko SATO<sup>2</sup>

<sup>1</sup>Department of Chemistry, Graduate School of Science, Kyoto University, Kyoto 606-8502

<sup>2</sup>Department of Physics, Chuo University, 1-13-27 Kasuga, Bunkyo-ku, Tokyo 112-8551

We report  $^7\text{Li}$  NMR studies of single crystals of triangular-lattice Heisenberg antiferromagnet  $\text{Li}_2\text{RuO}_6$ . Slow critical divergence with a wide critical region of  $|T - T_N| \lesssim 7$  K was observed in  $^7\text{Li}$  nuclear spin-lattice relaxation rate. The slowing down of staggered spin fluctuations was analyzed in a renormalized classical region of a two-dimensional triangular-lattice non-linear sigma model. A spin stiffness constant was found to reduce to about 20 % from the value in a spin-wave approximation. The effect of spin frustration, e.g.,  $Z_2$  vortex excitations on the critical phenomena is suggested.

KEYWORDS:  $\text{Li}_2\text{RuO}_6$ , triangular lattice, spin frustration, NMR, renormalized classical region

Spin frustration effect of a triangular lattice Heisenberg antiferromagnet has been one of the central issues in physics and chemistry of magnetic insulators. The ground state is classically a long range ordering state with the 120° spin structure, but the quantum mechanical ground state might be a gapped or gapless quantum spin liquid.<sup>1,3</sup> Elementary excitations of  $Z_2$  vortices, topologically stable point defects, are inherent even in classical triangular spin systems.<sup>4,7</sup> At finite temperatures, topological phase transition between the paramagnetic states is theoretically predicted from numerical simulations.

Finite-temperature magnetic long range ordering of quasi low dimensional antiferromagnets may be ascribed to a three dimensional interaction and the anisotropy. The low dimensional characteristics are (i) the suppressed magnetic ordering temperature  $T_N < T_N^{\text{MF}}$  in the mean field approximation, (ii) the suppressed Curie-Weiss law, i.e., the maximum of uniform spin susceptibility at  $T_{\text{max}}$  due to short range ordering, and (iii) a wide critical region in two dimensions.<sup>3</sup>

Two dimensional square lattice Heisenberg antiferromagnet has been intensively studied through the studies of high- $T_c$  cuprates.<sup>2,3</sup> Our understanding a short range ordering has made rapid progress. In the renormalized classical region, an antiferromagnetic correlation length and a staggered spin susceptibility diverge exponentially toward  $T_N = 0$  K,<sup>8,9</sup> which were observed in  $\text{La}_2\text{CuO}_4$ .<sup>10,11</sup> Such a wide critical region toward  $T_N = 0$  K is the notable feature of two dimensional square lattice Heisenberg antiferromagnets. Non-linear sigma model and field theoretical treatments turned out to be the relevant model and to give us powerful methods to describe the low energy excitations. They were also applied to the non-collinear frustrated magnetic systems like the triangular lattice.<sup>12,17</sup> To our knowledge, however, the theoretical critical behavior has not been widely tested to the actual critical phenomena of triangular spin systems.

A delafossite-type  $\text{Li}_2\text{RuO}_6$  has been at first reported as hexagonal  $\text{Li}_2\text{RuO}_6$ .<sup>18</sup> However, a detailed analysis on powder<sup>19</sup> and on single crystal<sup>20</sup> revealed that the actual composition is  $\text{Li}_2\text{RuO}_6$  and the structure is slightly distorted from an ideal hexagonal lattice.  $\text{Li}_2\text{RuO}_6$  is triclinic and has the superlattice structure of the Li deficiency in the double Li layers.<sup>20</sup> Figures 1(a) and 1(b) show the crystal structure and the triangular lattice, respectively. Single  $\text{Li}_2\text{RuO}_6$  layer and double Li layers are stacked with each other. The  $\text{Li}_2\text{RuO}_6$  layer consists of a triangular lattice of  $\text{RuO}_6$  octahedrons and a Li honeycomb lattice. The Li ions occupy 12 sites in the  $\text{RuO}_6$  layer and 30 sites in the Li deficient layers in unit cell, which are crystallographically inequivalent. For

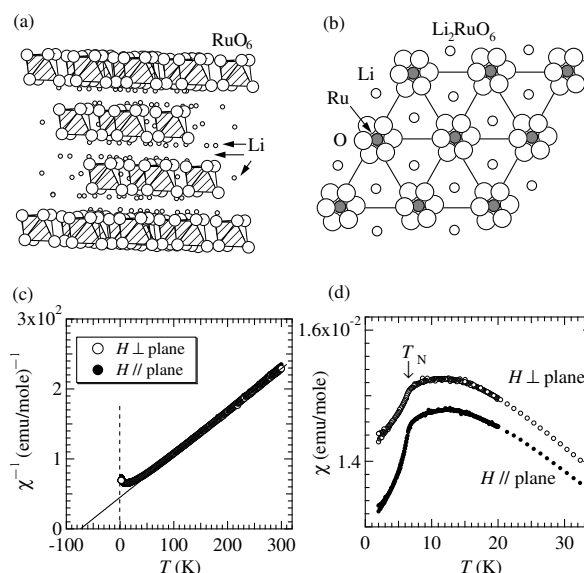


Fig. 1. (a) Schematics of crystal structure of  $\text{Li}_2\text{RuO}_6$  and (b) the top view of a triangular lattice Ru plane. (c) Inverse magnetic susceptibility  $\chi^{-1}$  and (d) the magnetic susceptibility of a single crystal  $\text{Li}_2\text{RuO}_6$ . The solid lines are the best fits by an inverse Curie-Weiss law. The arrow indicates  $T_N = 6.5$  K.

a hexagonal model of  $\text{Li}_2\text{RuO}_6$ , the staggered magnetic field from Ru would be cancelled out at the Ru-plane Li site. However, for the actual  $\text{Li}_2\text{RuO}_6$ , since the Li ions occupy non-ideal positions deviated from the center of the Ru triangle, then the 120° staggered spin fluctuations can be probed through the  $^7\text{Li}$  NMR.  $\text{Li}_2\text{RuO}_6$  is a deformed triangular lattice system. The detail of the crystal growth and the structure analysis will be published in a separated paper.<sup>20</sup>

Uniform magnetic susceptibility ( $\chi = k$  and  $\chi = ?$  denote  $H \parallel$  plane and  $H \perp$  plane) shows a slightly anisotropic Curie-Weiss behavior  $\chi = C/(T - \theta)$  with  $C = 1.89 \text{ emu/mol Ru}$  and  $\theta = 73 \text{ K}$  at high temperatures. Figures 1(c) and 1(d) show the inverse magnetic susceptibility  $1/\chi$  up to 300 K and the magnetic susceptibility  $\chi$  on an enlarged scale for a single crystal, respectively. Upon cooling,  $\chi$  makes a maximum at about 12.5 K and drops sharply at the Neel temperature  $T_N = 6.5 \text{ K}$ .<sup>19,20</sup> The broad maximum behavior indicates a low dimensional magnet. The Curie constant  $C$  is close to the value for  $S = 3/2$  and  $g = 2$ . For a Heisenberg spin Hamiltonian  $\sum_{nn} S_i \cdot S_j$  with the  $z$  nearest-neighbor exchange interaction  $J_{nn}$  between Ru ions, the Weiss temperature is given by

$$\theta = \frac{S(S+1)}{3} z J_{nn}; \quad (1)$$

in the mean field approximation. Using  $S = 3/2$  ( $\text{Ru}^{5+}$ ) and  $z = 6$ , we estimated the superexchange interaction  $J_{nn} = 9.7 \text{ K}$ . Since  $T_N = 6.5 \text{ K}$  and  $\theta = 73 \text{ K}$ , we obtain the ratio of  $T_N = |J|/J$   $\approx 0.089$ , which is nearly the same as 0.082 for  $\text{VCu}_2$  with  $S = 3/2$  ( $\text{V}^{4+}$ ).<sup>21</sup> These are the low dimensional characteristics of (i) and (ii). Thus, the layered compound  $\text{Li}_2\text{RuO}_6$  is a quasi-two dimensional antiferromagnet.

In this Letter, we report  $^7\text{Li}$  NMR studies of single crystals of triangular-lattice Heisenberg antiferromagnet  $\text{Li}_2\text{RuO}_6$ . We found slow critical divergence with a wide critical region of  $|T - T_N| > 7$  in  $^7\text{Li}$  nuclear spin-lattice relaxation rate, which is due to the slowing down of staggered spin fluctuations. From the analysis by renormalized classical fluctuations, we found the reduction of a spin stiffness constant, possibly due to the spin frustration effect.

Single crystals of  $\text{Li}_2\text{RuO}_6$  were grown from the mixture of  $\text{RuO}_2$  and a large amount of  $\text{Li}_2\text{CO}_3$  flux heated in an oxygen atmosphere at  $950^\circ\text{C}$ . Typically  $0.5 \times 0.5 \times 0.01 \text{ mm}$  sized and plate-like single crystals were obtained.<sup>20</sup> The plane and the vertical axes are confirmed to be the  $ab$  plane and the  $c$  axis of the quasi-hexagonal lattice, respectively. X-ray diffraction patterns for the powdered samples indicated the samples in a single phase. We performed  $^7\text{Li}$  (nuclear spin  $I = 3/2$  and nuclear gyromagnetic ratio  $\gamma_n = 2 \times 16.546 \text{ MHz/T}$ ) NMR spin-echo measurements at  $H = 7.48414 \text{ T}$  for the samples in which the several single crystal pieces were put on a plate. The NMR frequency spectra were obtained from Fourier-transformed spin-echoes or summing them at several frequencies and frequency-swept spin-echo intensity. The  $^7\text{Li}$  nuclear spin-lattice relaxation curves were measured by an inversion recovery technique and the relaxation

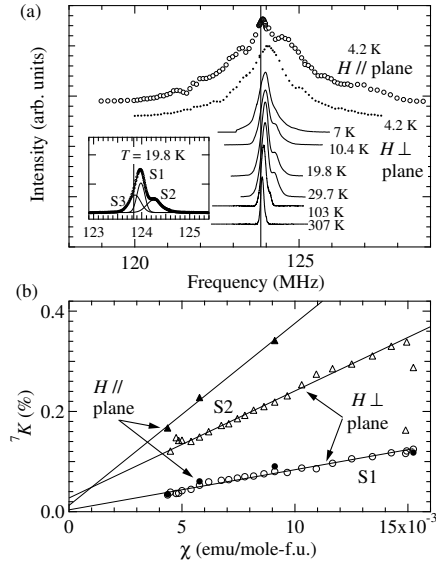


Fig. 2. (a)  $^7\text{Li}$  NMR frequency spectra of the single crystals of  $\text{Li}_2\text{RuO}_6$  at  $H \perp$  plane (solid curves and closed circles) and at  $H \parallel$  plane (open circles). The vertical line at 123.8343 MHz indicates the  $^7\text{Li}$  NMR spectrum peak of  $\text{LiCl}$  for a reference of zero shift. The inset shows the best fits by three Gaussian functions. (b) Knight shift  $^7K$  plotted against the bulk magnetic susceptibility  $\chi$  with temperature as an implicit parameter.

times  $T_1$ 's were obtained from the fits by a stretched exponential function of  $\exp[-(t/T_1)^\alpha]$  ( $t$  is the time after the inversion pulse).

Figure 2(a) shows  $^7\text{Li}$  NMR frequency spectra of the single crystals of  $\text{Li}_2\text{RuO}_6$  at  $H \perp$  plane (solid curves and closed circles) and at  $H \parallel$  plane (open circles). At

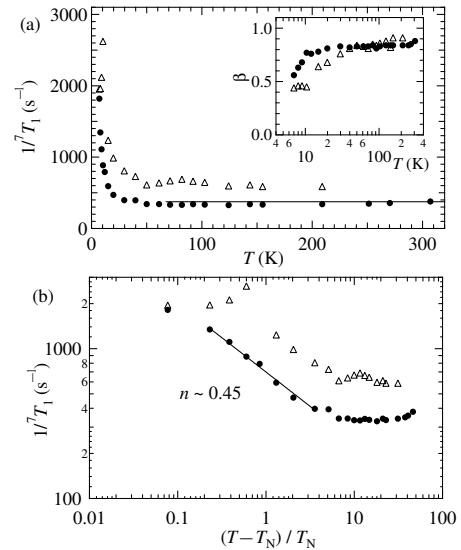


Fig. 3. (a) Temperature dependences of  $^7\text{Li}$  nuclear spin-lattice relaxation rates  $1/T_1$  of S1 (closed circles) and S2 (open triangles) at  $H \perp$  plane and  $T > T_N$ . The inset figure shows semi-log plots of the temperature dependences of the stretched exponents  $\alpha$ . (b) Log-log plots of  $^7\text{Li}$  nuclear spin-lattice relaxation rates  $1/T_1$  at  $H \perp$  plane against the reduced temperature  $(T - T_N)/T_N$ .

$T > 200$  K, a single sharp  $^7\text{Li}$  NMR spectrum and no quadrupole splits were observed. Upon cooling, the NMR spectrum shifts to higher frequency side and a weak signal separates and shifts more largely. At 4.2 K, both NMR spectra at  $H \parallel$  plane and  $H \parallel k$  plane are broadened nearly symmetrically. The featureless symmetric broadening below  $T_N$  indicates the emergence of internal magnetic field of an incommensurate staggered moments along the  $ab$  plane and the  $c$  axis.

The inset shows three Gaussian functions fit to the NMR spectrum at  $H \parallel$  plane and  $T = 19.8$  K. A sharp strong peak and a broad higher frequency peak are denoted by S1 and S2, respectively. S3 just adjusts the foot of the spectrum, whose Knight shift is 100 ppm and nearly independent of temperature. From the NMR intensity, the strong peak S1 and weak S2 can be assigned to the Li sites in the double Li layers and in the  $\text{RuO}_6$  triangle lattice layer, respectively. The assignment at  $H \parallel k$  plane at  $T > T_N$  not shown in Fig. 2(a) was less clear, since at least 4 peaks were observed. The lowest and highest frequency peaks are assigned to S1 and S2, respectively.

Figure 2(b) shows  $^7\text{Li}$  Knight shifts of S1 and S2 plotted against the bulk magnetic susceptibility with temperature as an implicit parameter. The bulk magnetic susceptibility is expressed by the sum of a temperature dependent spin susceptibility  $\chi_{\text{spin}}$ , the Van Vleck orbital susceptibility  $\chi_{\text{VV}}$ , and the diamagnetic susceptibility of inner core electrons  $\chi_{\text{dia}}$ . The  $^7\text{Li}$  Knight shift is expressed by  $K = A(i) \chi_{\text{spin}} / N_A \mu_B + K_{\text{dia}}$  ( $i = 1$  and 2 denote S1 and S2,  $N_A$  is Avogadro's number, and  $\mu_B$  is the Bohr magneton). From the  $K$  plots in Fig. 2, we obtained positive hyperfine coupling constants of  $A_k(1) = A_2(1) = 0.45$  kOe/ $\mu_B$ ,  $A_k(2) = 2.0$  kOe/ $\mu_B$  and  $A_2(2) = 1.2$  kOe/ $\mu_B$ . The positive  $A(1)$  and  $A(2)$  indicate the predominant role of a transferred hyperfine coupling.

Figure 3(a) shows temperature dependences of  $^7\text{Li}$  nuclear spin-lattice relaxation rates  $1/T_1$  of S1 and S2 at  $H \parallel$  plane and  $T > T_N$ . The inset figure shows semi-log plots of the temperature dependences of the stretched exponents  $\beta$ . At high temperatures,  $1/T_1$  levels off, which indicates the exchange narrowing limit. At low temperatures,  $1/T_1$  shows the divergence behavior due to the critical slowing down of the staggered spin fluctuations.

In general, the high temperature limit of  $1/T_1$  in the exchange narrowing is expressed by<sup>22</sup>

$$\frac{1}{T_{11}} = \frac{r}{2} \frac{S(S+1)}{3} \frac{2}{3} \frac{A_k^2}{\mu_B^2} \quad (2)$$

and

$$\beta_{\text{ex}}^2 = \frac{2}{3} z S(S+1) \left( \frac{k_B J_{nn}}{\mu_B} \right)^2 \quad (3)$$

The hyperfine field at the in-plane Li results from the 3 nearest neighbor Ru spins. The number of the nearest neighbor exchange coupled Ru spins is 6. Putting  $z = 6$ ,  $S = 3/2$ ,  $A_k(2) = 2.0$  kOe/ $\mu_B$  and  $J_{nn} = 9.7$  K for eqs. (2) and (3), we obtain  $1/T_{11} = 340$  s<sup>-1</sup>, which is the same order of magnitude but slightly smaller than the actual  $1/T_1 = 400$  and  $600$  s<sup>-1</sup> for S1 and S2 above 200

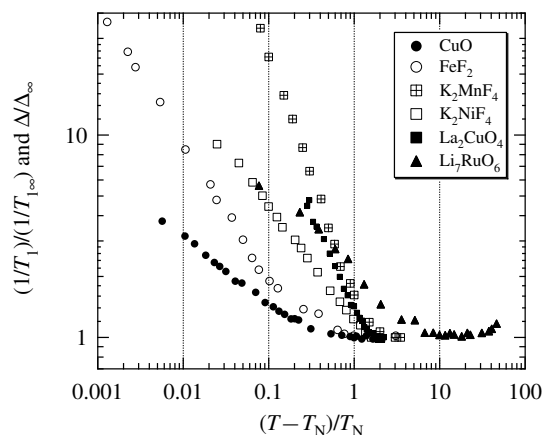


Fig. 4. Log-log plots of the nuclear spin-lattice relaxation rate  $(1/T_1)/(1/T_{11})$  or the continuous-wave (cw) NMR linewidth  $1/T_1$  against the reduced temperature  $(T - T_N)/T_N$  for the critical phenomena of  $\text{CuO}$ ,<sup>24</sup>  $\text{FeF}_2$ ,<sup>25</sup>  $\text{K}_2\text{MnF}_4$ ,<sup>26</sup>  $\text{K}_2\text{NiF}_4$ ,<sup>27</sup>  $\text{La}_2\text{CuO}_4$ ,<sup>10</sup> and  $\text{Li}_7\text{RuO}_6$  (S1). The circles, squares and triangles are three dimensional magnets, quasi two dimensional square lattices, and a triangular lattice, respectively. The solid and open symbols are the data by spin-echo and continuous-wave (cw) measurements, respectively.

K, respectively. The experimental value of  $T_1$  depends on the fitting function more or less. Using the fitting function of a double exponential function, we obtained a long component of  $1/T_1 = 277$  and  $435$  s<sup>-1</sup> for S1 and S2, respectively, being the same order of magnitude of the estimated  $1/T_{11}$ .

Figure 3(b) shows log-log plots of  $1/T_1$  against the reduced temperature  $(T - T_N)/T_N$ . The critical divergence of  $1/T_1$  starts from  $j = T_N - 1$  J. Although such a wide critical region is not usually regarded as a three dimensional critical region, we tried to apply a power law of  $j = (T - T_N)^n$  and then obtained  $n = 0.45$ . This is close to the mean field value.<sup>23</sup>

Figure 4 shows log-log plots of the nuclear spin-lattice relaxation rate  $(1/T_1)/(1/T_{11})$  or the continuous-wave (cw) NMR linewidth  $1/T_1$  against the reduced temperature  $(T - T_N)/T_N$  for the critical phenomena of  $\text{CuO}$ ,<sup>24</sup>  $\text{FeF}_2$ ,<sup>25</sup>  $\text{K}_2\text{MnF}_4$ ,<sup>26</sup>  $\text{K}_2\text{NiF}_4$ ,<sup>27</sup>  $\text{La}_2\text{CuO}_4$ ,<sup>10</sup> and  $\text{Li}_7\text{RuO}_6$ . The onset temperatures of the increase in  $T_{11}/T_1$  and linewidth  $1/T_1$  are the beginning of the critical slowing down of relevant spin fluctuations and indicate the width of the individual critical region. For a narrow critical region of  $j \ll 0.1$  of  $\text{CuO}$  and  $\text{FeF}_2$ , the critical exponent of three dimensional critical slowing down was estimated.<sup>24,25</sup> The wide critical region of  $j \sim 1.0$  of  $\text{La}_2\text{CuO}_4$  was successfully understood by a two dimensional short range ordering effect in the renormalized classical region of the square lattice.<sup>10</sup> The wide critical regions of square lattices  $\text{K}_2\text{MnF}_4$  and  $\text{K}_2\text{NiF}_4$  were also understood by the renormalized classical fluctuations.<sup>28,29</sup> The critical region of  $j \sim 7$  of  $\text{Li}_7\text{RuO}_6$  is wider than those of the two dimensional square lattice spin systems. One should note the another striking feature of the slow divergence of  $1/T_1$  of  $\text{Li}_7\text{RuO}_6$ . The wide but slow critical divergence of  $1/T_1$  characterizes

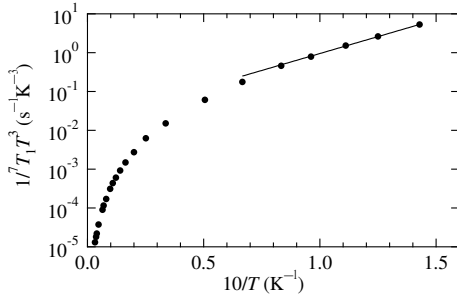


Fig. 5. Semi-logarithmic  $1/T_1 T^3$  against  $10/T$  for  $\text{Li}_7\text{RuO}_6$  (S1) at H-Q plane. The straight line is the fitting function of eq. (5).

the critical phenomenon of  $\text{Li}_7\text{RuO}_6$ .

For the frustrated quantum antiferromagnets, the non-linear sigma model description tells us the magnetic correlation length<sup>12,14,15</sup>

$$\xi \sim \frac{1}{\sqrt{P}} \exp(4\pi T) \quad (4)$$

with a spin stiffness constant  $P$  ( $= \chi$  and  $k$  plane) and the nuclear spin-lattice relaxation rate<sup>14,15</sup>

$$\frac{1}{T_1} \sim T^3 \exp(4\pi T) \quad (5)$$

The spin stiffness constant  $\chi$  is given by

$$\chi = \frac{P}{2} Z_2 S^2 \langle \mathbf{J} \mathbf{J} \rangle = 1.51 \langle \mathbf{J} \mathbf{J} \rangle \quad (6)$$

where a renormalization factor  $Z_2$  is estimated by a spin-wave approximation and  $1/S$  expansion.<sup>16,17</sup> Equations (4) and (5) are applicable to the low temperature states at  $T \sim 2$ .<sup>14,15</sup>

The NMR linewidth can serve as a probe of the magnetic correlation length in real space. The linewidth of the S2 NMR spectrum in Fig. 2(a) increased rapidly at 70 K upon cooling, which did not scale with the Knight shift  $K$  but was similar to the divergence in  $1/T_1$ . Thus, we may assume the temperature dependence as in eq. (4).

Figure 5 shows semi-logarithmic  $1/T_1 T^3$  against  $10/T$  for  $\text{Li}_7\text{RuO}_6$  at H-Q plane. The straight line is the fitting result of eq. (5). From the slope of the line at lower temperatures  $T < 15$  K, we estimated the exchange interaction  $\langle \mathbf{J} \mathbf{J} \rangle = 2.1$  K. Since  $2\chi = 20$  K, the fitting range is justified a posteriori. The interaction  $\langle \mathbf{J}_{nn} \mathbf{J} \rangle = 9.7$  K from the Weiss temperature reduces to  $\langle \mathbf{J} \mathbf{J} \rangle = 2.1$  K at low temperatures. Since  $J_{nn}$  should not strongly depend on temperature in the range of  $4.2 \text{ K} < T < 300 \text{ K}$ , the alternative reduction should trace back to the renormalization factor  $Z_2$  and the stiffness constant  $\chi$ .  $Z_2$  should reduce to about 20% from the value in the spin-wave approximation. This reduction might be the effect of the spin frustration, e.g., the topological  $Z_2$  vortex excitations on the spin correlation, which agrees with the numerical simulations.<sup>7</sup> The reduced  $Z_2$  and  $\chi$  are just to put the slow divergence of  $1/T_1$  in another way.

The wide critical region has been observed for the other  $S = 3/2$  triangular lattice systems such as  $\text{VCr}_2$ ,<sup>30</sup>  $\text{HCrO}_2$ ,<sup>31</sup> and  $\text{LiCrO}_2$ .<sup>31,32</sup> It is, however, less clear

whether the slow critical divergence is ubiquitous in the triangular lattices.

In conclusion, we found slow critical divergence with a wide critical region of  $|T - T_N| \sim 7$  in  $\text{Li}_7\text{RuO}_6$  nuclear spin-lattice relaxation rate for the triangular-lattice antiferromagnet  $\text{Li}_7\text{RuO}_6$ . We applied renormalized classical staggered spin fluctuations to the slow divergence and then obtained the reduction of a spin stiffness constant, suggesting the spin frustration effect.

We thank D. M. Ouhanna for valuable discussions. This work was supported in part by a Grant-in-Aid for Science Research on Priority Areas, "Invention of Anomalous Quantum Materials," from the Ministry of Education, Culture, Sports, Science and Technology of Japan (Grant No. 16076210) and in part by a Grant-in-Aid for Scientific Research from the Japan Society for the Promotion of Science (Grant No. 19350030).

- 1) P. W. Anderson: *Mat. Res. Bull.* **8** (1973) 153.
- 2) E. Fradkin: *Field Theories of Condensed Matter Systems* (Addison-Wesley Publishing Co. Tokyo 1991).
- 3) A. M. Tsvelik: *Quantum Field Theory in Condensed Matter Physics* (Cambridge University Press, New York 2003).
- 4) H. Kawamura and S. Miyashita: *J. Phys. Soc. Jpn.* **53** (1984) 9.
- 5) H. Kawamura and S. Miyashita: *J. Phys. Soc. Jpn.* **53** (1984) 4138.
- 6) S. Miyashita and H. Shiba: *J. Phys. Soc. Jpn.* **53** (1984) 1145.
- 7) M. Caraglio, P. A. Zaria, B. Delamotte, and D. M. Ouhanna: *Phys. Rev. B* **64** (2001) 014412.
- 8) S. Chakravarty, B. I. Halperin, and D. R. Nelson: *Phys. Rev. B* **39** (1989) 2344.
- 9) S. Chakravarty and R. Orbach: *Phys. Rev. Lett.* **64** (1990) 224.
- 10) T. Imai, C. P. Slichter, K. Yoshimura, and K. Kosuge: *Phys. Rev. Lett.* **70** (1993) 1002.
- 11) R. J. Birgeneau et al.: *Phys. Rev. B* **59** (1999) 13788.
- 12) P. A. Zaria, B. Delamotte, and D. M. Ouhanna: *Phys. Rev. Lett.* **68** (1992) 1762.
- 13) P. A. Zaria, Ph. Lecheminant, and D. M. Ouhanna: *Nucl. Phys. B* **455** (1995) 648.
- 14) A. V. Chubukov, S. Sachdev, and T. Senthil: *Phys. Rev. Lett.* **72** (1994) 2089.
- 15) A. V. Chubukov, S. Sachdev, and T. Senthil: *Nucl. Phys. B* **426** (1994) 601.
- 16) A. V. Chubukov, S. Sachdev, and T. Senthil: *J. Phys.: Condens. Matter* **6** (1994) 8891.
- 17) P. Lecheminant, B. Bernu, C. Lhuillier, and L. P. Pierre: *Phys. Rev. B* **52** (1995) 9162.
- 18) I. S. Shaplygin, M. I. G. Adzhiev, and V. B. Lazarev: *Russ. J. Inorg. Chem.* **32** (1987) 418.
- 19) C. Muhle, A. Karpov, A. Verhoeven, and M. Jansen: *Z. Anorg. Allg. Chem.* **631** (2005) 2321.
- 20) K. Nakajima and H. Sato: unpublished works.
- 21) K. Hirakawa, H. Ikeda, H. Kadowaki, and K. Ubukoshi: *J. Phys. Soc. Jpn.* **52** (1983) 2882.
- 22) T. Mori: *Prog. Theor. Phys.* **16** (1956) 23, *ibid.* 641.
- 23) T. Mori: *Prog. Theor. Phys.* **28** (1962) 371.
- 24) Y. Itoh, T. Imai, T. Shimizu, T. Tsuchida, H. Yasuoka, and Y. Ueda: *J. Phys. Soc. Jpn.* **59** (1990) 1143.
- 25) A. M. G. Ottlieb and P. Heller: *Phys. Rev. B* **3** (1971) 3615.
- 26) C. Bucci and G. Guidi: *Phys. Rev. B* **9** (1974) 3053.
- 27) E. P. M. Aarschall, A. C. Bottemann, S. Vega, and A. R. M. Iedema: *Physica* **41** (1969) 473.
- 28) Y. Itoh and K. Yoshimura: unpublished works.
- 29) R. J. Birgeneau: *Phys. Rev. B* **41** (1990) 2514.
- 30) H. Kadowaki et al.: *J. Phys. Soc. Jpn.* **56** (1987) 4027.
- 31) Y. Ajiro et al.: *J. Phys. Soc. Jpn.* **57** (1988) 2268.
- 32) L. K. Alexander et al.: *Phys. Rev. B* **76** (2007) 064429.